Available online at www.sciencedirect.com
ScienceDirect
Journal of the European Ceramic Society 30 (2010) 1345–1350
www.elsevier.com/locate/jeurceramsoc

Surface texturing inside ceramic macro/micro channels

David Salamon, Rob G.H. Lammertink *, Matthias Wessling

Membrane Technology Group, Faculty of Science and Technology, Mesa+ Institute for Nanotechnology, University of Twente, P.O. Box 217, NL-7500 AE Enschede, The Netherlands

Received 13 August 2009; received in revised form 30 October 2009; accepted 17 November 2009
Available online 9 December 2009

Abstract

Surface textures (roughness) inside of macro/micro channels have a number of potential uses in advanced ceramic applications, including areas such as bioceramic, cooling, microreactors or friction control. The presented microtemplating method is dealing with templating of structured fibres, which results in formation of variation in surface textures and roughness. Effect of the microtemplate skin texture and ceramic slurry behaviour has been investigated and discussed. Porosity and defects of the microtemplate skin play a key role for roughness/texture of sintered microchannels if their size is larger than the ceramic grain size. The surface roughness inside the micro/macro channel can be easily changed from $R_a = 0.8\ \mu m$ to $R_a = 4.9\ \mu m$ just by changing the microtemplate skin porosity. The results demonstrate possibilities to use this method to tailor surface texture inside microchannels in a one step procedure.

Keywords: Surfaces; Al_2O_3; Structural applications; Microtemplating

1. Introduction

Internal microchannels are used to transport fluids in many diverse technological applications. Microfluidic science and technology process or manipulate small amount of liquids, using channels with dimensions of tens to hundreds of micrometers. Ceramics have several desired properties for microfluidic systems, e.g., heat resistance, hardness and corrosion resistance. This paper focuses on controlling the surface texture inside ceramic channels. The surface texture/roughness has increasing influence with decreasing scale of the systems.[1] Areas where textured surface is considerable include bioceramics, microstructured heat exchangers, and wear applications. Textured scaffold surface of hydroxyapatite is important for tissue regeneration, regarding bone growth into an implant material (ossointegration).[2] A microstructure heat exchanger has promising areas of application in laboratory and industry.[3] Many electronic devices suffer from increased heat production when size decreases and requires an active cooling. Surface roughness is increasing turbulence mixing near the channel wall that in turn increases the heat transfer coefficient.[4] Friction control is another field of surface engineering. Surface microtexture reduces friction during running-in, and also improves the long-term wear behaviour. The poorer running-in behaviour of oxide ceramics compared to non-oxide ceramics in water can be overcome by surface engineering.[5]

Nowadays preparation of textured ceramic microchannels is in many cases done with silicon technology methods. Preparation of microchannels requires two process steps. The first step of the process is machining,[6,7] pressing or stamping channels,[8] or burning out fugitive template.[9] The second step concerns the ceramic/ceramic joining. The fabrication is relatively expensive, time consuming and usually does not produce rounded shapes of microchannels.[10] Alternative routes use a ceramic plastic process[11] together with templated grain growth (TGG),[12] but variability of possible surface textures is limited to grain size dimensions.

In this study we are using our microtemplating method[13] which was recently developed. The controlled dip-coating of a sacrificial polymeric fibre template with suspensions containing sinterable particles is the basis for the microtemplating method. The template is sacrificed during a subsequent firing stage. We have used differently structured microtemplate (fibres) to modify the surface texture and roughness of the sintered macro/micro

* Corresponding author. Tel.: +31 53 489 2063; fax: +31 53 489 4611.
E-mail address: r.g.h.lammertink@utwente.nl (R.G.H. Lammertink).

0955-2219/$ – see front matter © 2009 Elsevier Ltd. All rights reserved.
doi:10.1016/j.jeurceramsoc.2009.11.011

Table 1
Compositions of the microtemplating slurries.

Material	Function	*A* Quantity (wt.%)	*B* Quantity (wt.%)
Al_2O_3 powder (Sumitomo Chemical, AKP-15, $d_{50} = 600$ nm)	Ceramic phase	58	38
MgO powder (Alfa Aesar, 100 nm APS, S.A. > 7.3 m^2/g)	Ceramic phase	–	5
2-Propanol	Suspending medium	34	47
Solperse 20000 (±90% polymeric alkoxylate)	Dispersant	3	4
PVB (polyvinyl butyral) B-98	Binder	4	6
BBP (benzyl butyl phthalate), S-160	Plasticizer	1	1

Table 2
Characteristic of the microtemplate fibres.

#	Fibre	Outer diameter (μm)	Skin	Structure of the skin
1	Macroporous PP fibre	2730	Open, pore size < 20 μm	Bridges between pores
2	Microporous PP fibre	300	No porosity	Vertical defect
3	Hair	80	No porosity	Fine pattern
4	Polyimide (P84)	970	Open, pore size < 0.300 μm	Local defects
5	Polyimide (P84)	310	No porosity	Fine defects

channels. Our method allows one step texturing of microchannels economically and fast. Limits and flexibility of this method are also demonstrated here.

2. Experimental

Two alcohol-based slurries with different compositions and viscosity were selected to demonstrate the texture procedure inside ceramic microchannels via microtemplating. The ceramic slurries were prepared by ball milling (5 mm YSZ) for 24 h. Submicron alumina powder (AKP-15) is used for the suspension *A*. The suspension has high loading and dynamic viscosity ($\mu = 0.27 \pm 0.02$ Pa s). Suspension *B* contains, beside alumina submicron powder, also magnesia nano powder as minor ceramic phase. The suspension loading and dynamic viscosity ($\mu = 0.19 \pm 0.01$ Pa s) are lower compared to *A* suspension. The suspensions have shear thinning behaviour, which is significant only for shear rate below 10 s^{-1} (HAAKE, RheoStress 600). Compositions and function of additives are summarized in Table 1.

Prepared suspensions were used for multiple dip-coating of selected fibres (serving as microtemplate). Dimensions and characterization of the template surface are given in Table 2. All fibres except no. 3 (hair) have hollow and porous internal structure, which is the most suitable internal structure for the microtemplating method. The skin structure of the fibres is described in Table 1 and shown on SEM figures (Figs. 1 and 2, left). The fibres withdrawing velocity from the suspensions was set constantly at 0.29 m min^{-1}. The velocity provides shear rate high enough to minimize shear thinning of the prepared suspensions and keep dip-coating conditions stable for all fibre diameters. The dip-coating procedure was repeated 6-times (for fibre no. 3 due to small diameter 8-times) to obtain a wall thickness, which after sintering is strong enough to self-support the structure. Drying of dip-coated layer takes at least 10 min between two steps. All samples were dried at room temperature 24 h before heat treatment.

Green samples were calcined and sintered in one heating procedure in a high temperature furnace (Nabartherm LHT 04/17). Air atmosphere without forced circulation was used. Two heat treatment processes were used with different sintering temperatures of 1300 °C and 1600 °C. The heat treatment procedures had equal heating steps, 5 °C min^{-1} to 220 °C, 0.5 °C min^{-1} to 460 °C, 5 °C min^{-1} to 600 °C, 10 °C min^{-1} to a final sintering temperature of 1300 °C or 1600 °C. The sintering temperature was held for 4 h, and then the furnace was cooled down at 5 °C min^{-1} to 25 °C.

Table 3
Characteristic of ceramic macro/micro channels after sintering.

#	*A*—inner diameter (μm) 1300/1600 °C [weight (g/m)]	*B*—inner diameter (μm) 1300/1600 °C [weight (g/m)]	Inner texture
1	2540/2330 [17.8]	2690/2240 [8.1]	Cross hatched pattern open porosity
2	280/260 [3.4]	300/250 [1.3]	Smooth surface, vertical defect in grain aliment
3	70/70 [2.5]	80/70 [0.6]	Smooth surface, no significant pattern
4	900/830 [8.8]	960/800 [3.1]	Smooth surface, local roughness on micrometers level
5	290/260 [2.8]	310/250 [1.6]	Smooth surface, open pores on surface

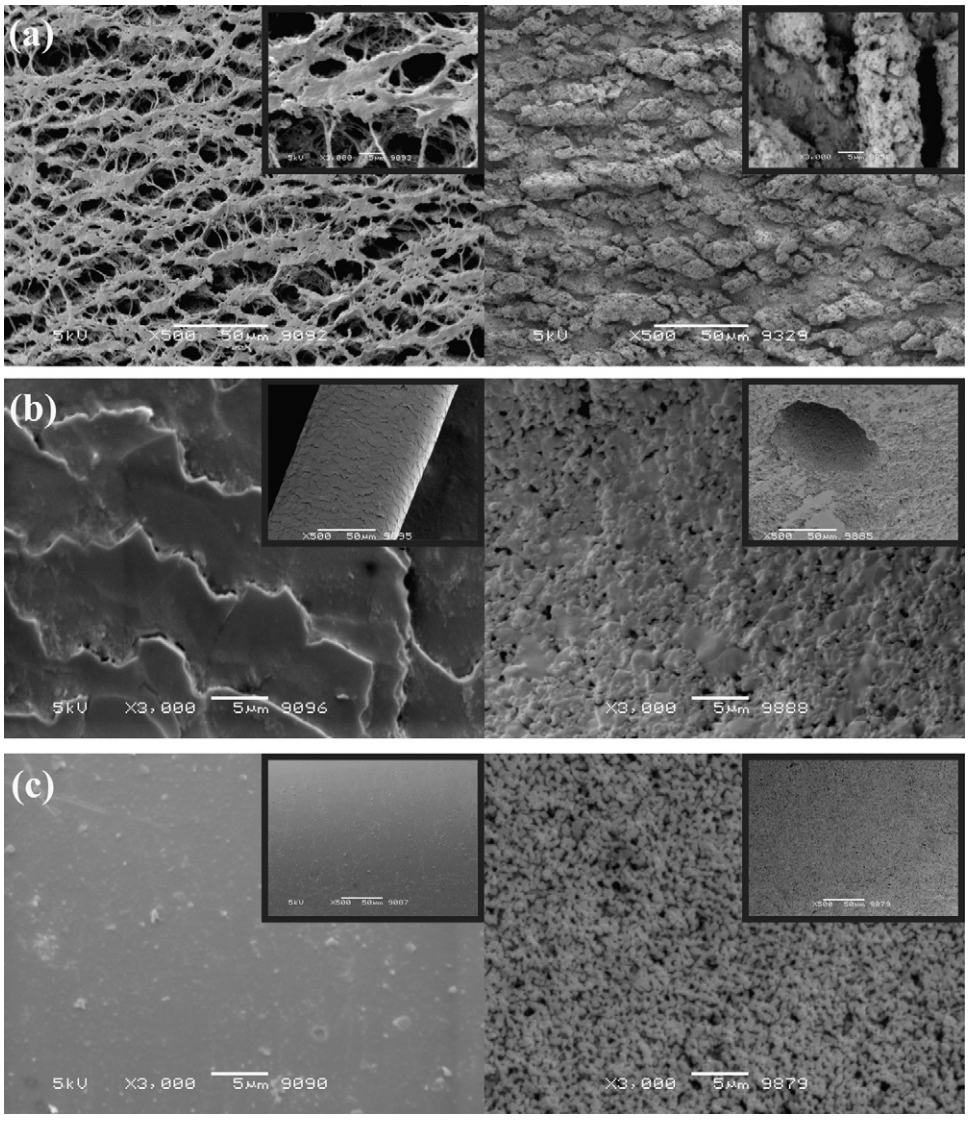

Fig. 1. SEM images of the templates skin (left) and inner wall of templated ceramic channels (right), (a) template 1 microtemplated by suspension *A* and sintered at 1600 °C, (b) template 3 microtemplated by suspension *B* and sintered at 1600 °C, (c) template 5 microtemplated by suspension *B* and sintered at 1300 °C.

The microstructures and textures of the samples were characterized with scanning electron microscopy (Jeol JSM 5600LV). SEM samples were prepared by cutting with diamond disk and cleaned with an ultrasonic stirrer. The surface roughness of the selected samples was quantified by scanning confocal microscope (Sensofar PLu neox). The presented roughness was measured in the flow direction of the micro/macro channel to eliminate an influence of the channel deflection. Density of a sample was measured by helium pycnometry (AccuPyc 1330 pycnometer).

3. Results and discussions

Mechanically stable macro/micro channels with different surface roughness and varying porosity were prepared. A description of the sintered macro/micro channels is given in Table 3. The surface roughness of selected sintered macro/micro channels prepared from composition A and sintered at 1600 °C is quantified in Table 4. The influence of the ceramic slurry composition, green microtemplate structure, and sintering conditions on formation of the ceramic micro/macro channels texture is investigated.

3.1. Composition and temperature effect

Compositions of ceramic slurry and sintering temperatures play a major role in the sintering of microtemplated samples. Ceramic slurry *A* is a stable suspension with relatively high ceramic load. The volume shrinkage during the sintering was 7% at the sintering temperature of 1300 °C and 15% at the sintering temperature of 1600 °C. The relative density of the sintered sample reached 96% of the theoretical density (3.97 g cm^{-3}) at the sintering temperature of 1600 °C. The residual 4% of porosity is the closed porosity. Composition *B* contains MgO which prevents densification under the current sintering conditions. The volume shrinkage is only around 1% at the sintering temperature

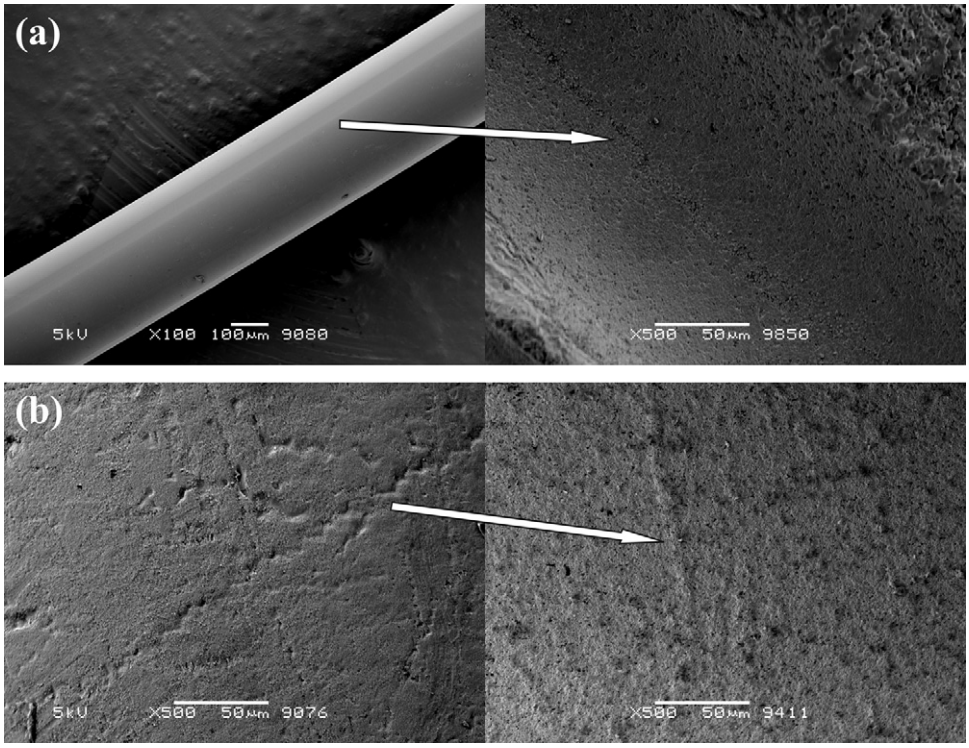

Fig. 2. SEM micrographs focused on defects of the templated structure (left) and their transfer to inner ceramic wall (right); (a) template 2 microtemplated by suspension *A* and sintered at 1600 °C, (b) template 4 microtemplated by suspension *B* and sintered at 1600 °C. White arrow shows effect of defects, black arrow shows inner surface porosity.

of 1300 °C, and significantly increases to 18% at the sintering temperature of 1600 °C. The final microstructure is still porous and open in contrast to composition *A*. The presence of pores with high coordination number (Fig. 2b) in composition *B* and the shrinkage behaviour indicates that the green density of the coated layer of suspension *B* (Al_2O_3 + MgO) is lower compared to suspension *A* (Al_2O_3).

3.2. Microtemplate shape

Presented microtemplates are easily accessible and used in membrane technology applications (except hair—3), when porosity of the skin is the critical parameter. Individually tested (defect free) fibres are commercially available, but for demonstration purposes we have used fibres with surface defects caused by preparation techniques and manipulation.

Template 1 has the most open surface skin structure, containing pores in the range of micrometers. The very open skin structure allows intrusion of suspensions in range of micrometers that replicate the templated structure. The intrusion is limited by properties of the ceramic slurry. Solidification of alcohol-base ceramic slurry is very fast due to rapid evaporation of alcohols. Drying of ceramic slurry in the open structure of template 1 rapidly increases dried surface of the ceramic slurry. Viscosity difference between suspension *A* and *B* do not bring significant difference in the ceramic slurry penetration into the template 1. However, the viscosity is assumed to be important. Due to the open porous structure of the PP template fibre, melting of PP (≈200 °C) results in the shrinkage of templated fibre inside the hollow space. At the PP melting temperature, hardening of the binder and plasticizer ensures the structure. The template 1 structure (macroporous PP fibre), and resulting textured alumina structure (R_a = 4.9 μm) after sintering are shown in Fig. 1a.

In contrast to the open porous structure, the dense skin of hair (no. 3) contains a very fine pattern on the surface. We did not find any significant replication of this fine pattern, due to the grain size of the used suspensions. The templating of human hair resulted in smooth surface, where roughness is mainly determined by the ceramic slurry used for coating. Composition *B* gives a rougher surface due to the higher porosity and lower

Table 4
Quantification of the surface roughness of selected macro/micro channels prepared from composition *A* and sintered at 1600 °C.

#	Surface	Maximum valley depth R_v (μm)	Root mean square roughness R_{RMS} (μm)	Average roughness R_a (μm)
1	Inside	19.645	5.732	4.939
2	Inside	7.417	1.262	0.838
1	Outside	0.593	0.141	0.117
2	Outside	0.629	0.117	0.088

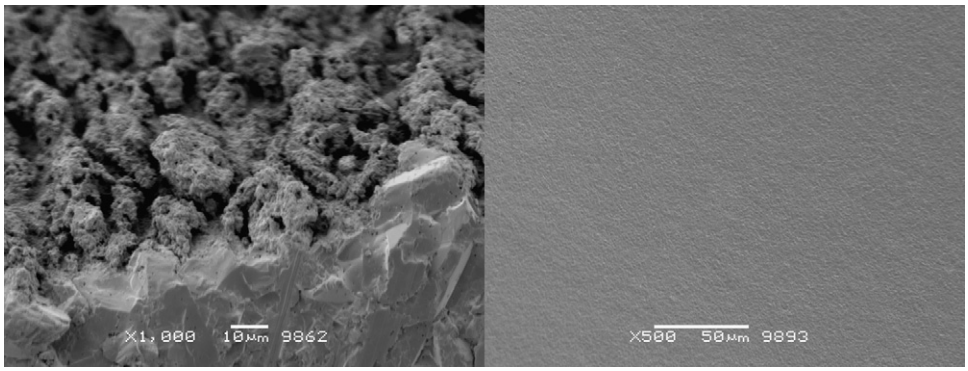

Fig. 3. SEM cross-section view (left) of the textured macro channel (template 1, suspension *A*, sintering temperature 1600 °C) in contrast of the smooth outside surface (right).

homogeneity of the suspension (due to two different particle sizes). Nevertheless, the inner surface is very smooth compared to template 1, Fig. 1b.

Template 5 also has a dense skin, but with small randomly distributed defects in size comparable to the ceramic grain size. The porosity of a microchannel templated with ceramic slurry *B* did not show significant influence of these defects compared to a free dried (outside) surface. Channel microtemplated with slurry *A* contains significantly more pores on the surface compared to a free dried surface. This phenomena was also observed for template 2 (Fig. 2a), when fine defects are not present. Pores in the inner surface are more likely connected with viscosity and dip-coating conditions. A preparation of the porous structures is not significantly effected and the smooth porous surface may be easily prepared inside the microchannel, Fig. 1c.

The surface defects may also be in the range of micrometers and then have already significant influence on templated structures. Microtemplates originated from membrane technology applications may contain two kinds of skin defects. A "vertical line" (Fig. 2a) is the relict of a processing tool (e.g., spinneret) and usually does not effect the skin porosity. This defect results in different particle alignment during the microtemplating procedure (Fig. 2a). The measured average surface roughness is in this case low ($R_a = 0.835\ \mu m$), whereas the maximal valley depth is relatively high ($R_v = 7.417\ \mu m$). The second kind of defect is localized and often randomly oriented and it usually is a residue of washing and mechanical manipulation. The localized defects result in localized increase of roughness or formation of local patterns after microtemplating. Fig. 2b shows replication these local micrometer range defects inside the ceramic microchannels.

Obviously, what we are presenting as a defect may be used to tailor internal texture of microchannels. The present methods are very developed to shape surfaces and relatively easily textured polymeric surface can be used to shape the inside surface of ceramic microchannels. Tailoring of ceramic slurry properties (especially viscosity and evaporation) allows to prepare functionally gradient material, where porosity may be introduced just by the drying procedure during dip-coating step, see Fig. 3. The textured porous structure inside the channel is in contrast to the dense and smooth surface outside ($R_a = 0.117\ \mu m$), when both are prepared in one step procedure from the same ceramic slurry.

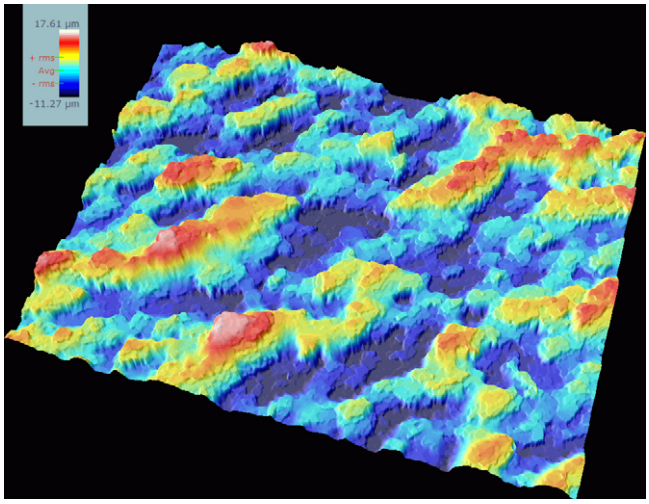

Fig. 4. Scanning confocal microscope image demonstrating the roughness character of the sintered ceramic microchannel prepared by microtemplating using template 1 with the composition *A*; sintered at 1600 °C.

The surface roughness stems not primarily from the porosity, but rather from the templating (Fig. 4).

4. Conclusions

We have demonstrated an original method for micro texturing of macro/micro channels surface. The results presented show that textured patterns depend mainly on the shape of a microtemplate. Porosity, defects and errors of the microtemplate skin play a key role for roughness of the sintered microchannels only if their size range is larger than the grain size of a ceramic phase. Presented examples show a possibility to prepare significantly textured structures in a controlled way. Future possibilities of tailoring polymeric microtemplates to design ceramic microchannels with tailored textures or roughness are obvious from the presented results.

Acknowledgement

The Dutch Technology Foundation (STW) is gratefully acknowledged for the financial support. We thank B. Pathiraj for the Scanning confocal microscope results. Gor

Manukyan is acknowledged for help with the viscosity measurements.

References

1. Taylor JB, Carrano AL, Kandlikar SG. Characterization of the effect of surface roughness and texture on fluid flow—past, present, and future. *International Journal of Thermal Sciences* 2006;**45**:962–8.
2. Wilson CE, de Bruijn JD, van Blitterswijk CA, Verbout AJ, Dhert WJA. Design and fabrication of standardized hydroxyapatite scaffolds with a defined macro-architecture by rapid prototyping for bone-tissue-engineering research. *Journal of Biomedical Materials Research Part A* 2004;**68A**:123–32.
3. Brandner JJ, Bohn L, Henning T, Schygulla U, Schubert K. Microstructure heat exchanger applications in laboratory and industry. *Heat Transfer Engineering* 2007;**28**:761–71.
4. Kang HJ, Wong TT, Leung CW. Effects of surface roughness on forced convection and friction in triangular ducts. *Experimental Heat Transfer* 1998;**11**:241–53.
5. Zum Gahr KH, Mathieu M, Brylka B. Friction control by surface engineering of ceramic sliding pairs in water. *Wear* 2007;**263**:920–9.
6. Etsion I. State of the art in laser surface texturing. *Journal of Tribology-Transactions of the Asme* 2005;**127**:248–53.
7. Dam H, Quist P, Schreiber MP. Productivity, surface quality and tolerances in ultrasonic machining of ceramics. *Journal of Materials Processing Technology* 1995;**51**:358–68.
8. Moran PM, Lange FF. Microscale lithography via channel stamping: relationships between capillarity, channel filling, and debonding. *Applied Physics Letters* 1999;**74**:1332–4.
9. Draeger DJ, Case ED. Engineering the surface texture and shape of channels in ceramic substrates. *Materials Science and Engineering B-Solid State Materials for Advanced Technology* 2003;**97**:94–105.
10. Lee JG, Shin HW, Case ED, Kwon P. The fabrication of smooth, submillimeter open channels and internal channels in ceramics and ceramic composites without machining. *Journal of Materials Science Letters* 2001;**20**:107–9.
11. Blackburn S, Wilson DI. Shaping ceramics by plastic processing. *Journal of the European Ceramic Society* 2008;**28**:1341–51.
12. Snel MD, van Hoolst J, de Wilde A-M, Mertens M, Snijkers F, Luyten J. Influence of tape cast parameters on texture formation in alumina by templated grain growth. *Journal of the European Ceramic Society* 2009, doi:10.1016/j.jeurceramsoc.2009.1003.1025.
13. Salamon D, Chlup Z, Lefferts L, Wessling M, Lammertink RGH. Ceramic free standing 3D microchannel structures designed via microtemplating. *Journal of the American Ceramic Society*, submitted.